



ORIGINAL PAPER

Marzia Sara Vaccaro · Raffaele Barretta ·  
Francesco Marotti de Sciarra · Junuthula N. Reddy

# Nonlocal integral elasticity for third-order small-scale beams

Received: 12 November 2021 / Revised: 31 January 2022 / Accepted: 4 April 2022 / Published online: 28 May 2022  
© The Author(s) 2022, corrected publication 2022

**Abstract** Small-scale beams are basic structural components of miniaturized electro-mechanical systems whose design requires accurate modeling of size effects. In this research, the size-dependent behavior of nonlocal elastic beams is investigated by adopting the stress-driven elasticity theory. Kinematics of beams is modeled by the Reddy variational third-order beam theory accounting for the effective distribution of shear stresses on cross sections without needing the evaluation of shear correction factors. Stress-driven integral elasticity is thus extended to third-order small-scale beams providing an equivalent constitutive formulation with boundary conditions. The relevant nonlocal elastic equilibrium problem is formulated and an analytical strategy is proposed to obtain closed-form solutions. The present approach is elucidated by solving some structural problems of current interest in Nanotechnology.

## 1 Introduction

There exist several one-dimensional theories in the scientific literature to model beams assuming different kinematic hypotheses [23]. Among these theories, the oldest and simplest model is the Bernoulli–Euler beam. According to this theory, cross sections are rigid plane bodies clamped to the beam axis. Thus, transverse shear strains are consequently neglected, which is a valid assumption to capture the structural behavior of slender beams.

A refined theory that is usually applied to model thick beams is the Timoshenko beam theory, also known as the first-order shear deformation theory [21]. This model is based on the kinematic hypothesis that cross sections are rigid planes attached to the beam axis. Thus, transverse shear strains are not neglected but they are uniform along the bending axis of cross section. Thus, a shear correction coefficient is needed to account for the effective distribution of shear stress.

A more refined model is the third-order shear deformation theory which assumes warping of cross sections [3, 10, 13, 20, 23, 24]. This higher-order beam theory accommodates quadratic variation of transverse shear strains and ensures the fulfillment of equilibrium boundary conditions. Hence, in the framework of the third-order theory there is no need to evaluate shear correction coefficients. Kinematics of the third-order shear deformation beam theory was first proposed by Levinson [13]. In 1984, a variationally consistent formulation was independently derived by Reddy [20].

The above-mentioned one-dimensional continuum theories can be efficiently adopted to model structural elements of new generation small-scale devices [2, 11, 16, 19, 32, 33], provided that size effects are properly

---

M. S. Vaccaro (✉) · R. Barretta · F. Marotti de Sciarra  
Department of Structures for Engineering and Architecture, University of Naples Federico II, via Claudio 21, 80125 Naples, Italy  
E-mail: marziasara.vaccaro@unina.it

J. N. Reddy  
J. Mike Walker '66 Department of Mechanical Engineering, Texas A&M University, College Station, TX 77843-3123, USA

taken into account in the constitutive law [14, 15]. Indeed, in modeling and design of micro- and nano-electro-mechanical systems (M/NEMS), nonlocal models of elasticity based on a continuum mechanics approach can be conveniently adopted in place of atomistic methodologies in order to reduce computational efforts.

Seminal contributions on nonlocal theories of continua can be found in [12, 26, 27]. A nonlocal model of elasticity based on a strain-driven integral approach was later exploited by Eringen to efficiently solve screw dislocation and wave propagation problems involving unbounded domains [5–7]. However, some issues emerged when the strain-driven model is applied to structural elements. Indeed, when applied to bounded domains, Eringen’s theory leads to an ill-posed nonlocal elastic problem due to incompatibility between constitutive and equilibrium equations [29, 30].

A well-posed nonlocal model based on a stress-driven integral approach has been recently proposed in [28] and it has been proven to be able to efficiently capture the size-dependent behavior of small-scale structures [4, 8, 17, 25, 31, 35]. According to the nonlocal stress-driven model, elastic strain at a point of a continuum depends on the stresses at all the other points by means of an integral convolution with a proper averaging kernel.

It is worth noting that in modeling of small-scale beams, a crucial point is the evaluation of the shear correction factor since an energetic equivalence must be prescribed between the Timoshenko beam and the three-dimensional Cauchy continuum. This issue can be overcome by adopting a third-order theory, that accommodates quadratic distribution of shear strain field and thus does not require shear correction coefficients.

In the present study, the nonlocal stress-driven elasticity [28] is combined with the Reddy variational third-order beam model [10, 20, 23, 24]. The plan of the paper is as follows: in Sect. 2, kinematics and equilibrium of the Reddy variational beam theory are illustrated; then, in Sect. 3 the nonlocal stress-driven elasticity is formulated for third-order beams; in Sect. 4, the nonlocal elastic equilibrium problem is analytically derived and an effective solution strategy is proposed. Finally, in Sect. 5 some case studies are investigated providing parametric closed-form solutions. Main outcomes of the present study are summarized in Sect. 6.

## 2 Kinematics and equilibrium of third-order beams

Let us consider a Cauchy three-dimensional continuum  $\mathcal{B}$  shaped as a right prism of length  $L$  with cross section modeled by a two-dimensional domain  $\Omega$ . The following coordinate system will be adopted: the  $x$ -axis, identified by the unit vector  $\mathbf{i}$ , is coincident with the locus of geometric centroid of cross sections; the  $y$ - and  $z$ -axes identify the plane of cross section and are associated to the unit vectors  $\mathbf{j}$  and  $\mathbf{k} := \mathbf{i} \times \mathbf{j}$ , respectively.

In a geometrically linearized theory, the kinematics of the continuum  $\mathcal{B}$  is assumed to be described by the following vector field [3, 10, 13, 20, 24]

$$\mathbf{u}(x, y, z) = \left[ -y \varphi(x) - \alpha y^3 \left( w'(x) - \varphi(x) \right) \right] \mathbf{i} + w(x) \mathbf{j}, \tag{1}$$

where the symbol  $(\bullet)'$  stands for first derivative along the  $x$ -axis. In Eq. (1), the function  $w(x)$  is the transverse displacement  $u_y$  of cross section along the  $y$ -axis while the function  $\varphi$  is defined as  $-\frac{\partial u_x}{\partial y} \Big|_{y=0}$ . The axial displacement  $u_x$  is composed of a linear (first-order) field along the  $y$ -axis and a third-order field along  $y$  representing the warping of cross section. The transverse displacement along  $z$  is assumed to be zero (because bending in the  $xy$ -plane is considered). The coefficient  $\alpha$  in Eq. (1) is equal to  $4/(3h^2)$ , where  $h$  is the maximum dimension of cross section along the  $y$ -axis. By computing the gradient of the displacement field in Eq. (1), we obtain

$$[\nabla \mathbf{u}] = \begin{bmatrix} -y \varphi' - \alpha y^3 (w'' - \varphi') & -\varphi - 3\alpha y^2 (w' - \varphi) & 0 \\ w' & 0 & 0 \\ 0 & 0 & 0 \end{bmatrix}. \tag{2}$$

Then, the total strain field  $\mathbf{D}$  is obtained by the kinematic compatibility formula  $\mathbf{D} = \text{sym } \nabla \mathbf{u}$ . Assuming  $\beta = 3\alpha$ , the nonzero strain components of  $[\mathbf{D}]$  are expressed as

$$\begin{cases} \varepsilon_x = -\bar{\varepsilon}(x) y - \bar{\bar{\varepsilon}}(x) y^3, \\ \gamma_{xy} = \bar{\gamma}(x) + \bar{\bar{\gamma}}(x) y^2, \end{cases} \tag{3}$$

where

$$\begin{cases} \bar{\varepsilon} := \varphi', \\ \bar{\gamma} := w' - \varphi, \\ \bar{\bar{\varepsilon}} := \alpha \bar{\gamma}', \\ \bar{\bar{\gamma}} := -\beta \bar{\gamma}. \end{cases} \tag{4}$$

Prescription of the variational equilibrium condition [22] together with the following static equivalences

$$\begin{vmatrix} M \\ P \end{vmatrix} = \int_{\Omega} -\frac{y}{y^3} \sigma_x \, dA, \quad \begin{vmatrix} Q \\ R \end{vmatrix} = \int_{\Omega} \frac{1}{y^2} \tau_{xy} \, dA \tag{5}$$

leads to the differential equilibrium equations  $\forall x \in [0, L]$

$$\begin{cases} \beta R'(x) - Q'(x) + \alpha P''(x) = q(x), \\ \alpha P'(x) - M'(x) + \beta R(x) - Q(x) = 0, \end{cases} \tag{6}$$

where  $P$  and  $R$  denote the higher-order stress resultants and  $q$  represents the distributed transverse loading. Equation (6) is equipped with the following boundary conditions:

$$\begin{cases} (Q - \beta R - \alpha P')(x_i) \delta w(x_i) = (-1)^i \mathcal{F}_i \delta w(x_i), \\ \alpha P(x_i) \delta w'(x_i) = (-1)^i \alpha \mathcal{P}_i \delta w'(x_i), \\ (M - \alpha P)(x_i) \delta \varphi(x_i) = (-1)^i \mathcal{M}_i \delta \varphi(x_i), \end{cases} \tag{7}$$

where  $i = \{1, 2\}$  with  $x_1 := 0, x_2 := L$ . In Eq. (7), virtual kinematic fields fulfilling homogeneous kinematic boundary conditions are denoted by  $\delta w, \delta \varphi, \delta w'$  while  $\mathcal{F}_i, \mathcal{M}_i, \mathcal{P}_i$  are concentrated forces and couples and higher-order concentrated couples.

As shown in Eq. (3)<sub>2</sub>, the shear strain  $\gamma_{xy}$  is a quadratic field on cross section and satisfies the zero condition at the lower and upper fibers. Hence, unlike the shear stress field provided by the Timoshenko beam theory, that is uniform and thus requires the introduction of a shear correction factor, on the contrary, there is no need to evaluate shear correction coefficients according to the third-order beam theory.

### 3 Nonlocal integral elasticity: the stress-driven model

Let us recall the constitutive equations of local elasticity for the plane and linearized third-order beam theory [24]. Denoting by  $E$  and  $G$  the Euler–Young and shear moduli, respectively, the stress resultants in Eq. (5) are related to local elastic strains by the following relation:

$$\begin{vmatrix} M \\ P \\ Q \\ R \end{vmatrix} = \begin{bmatrix} I_E^{(2)} & I_E^{(4)} & 0 & 0 \\ I_E^{(4)} & I_E^{(6)} & 0 & 0 \\ 0 & 0 & I_G^{(0)} & I_G^{(2)} \\ 0 & 0 & I_G^{(2)} & I_G^{(4)} \end{bmatrix} \begin{vmatrix} \bar{\varepsilon} \\ \bar{\bar{\varepsilon}} \\ \bar{\gamma} \\ \bar{\bar{\gamma}} \end{vmatrix}, \tag{8}$$

where

$$I_E^{(m)} := \int_{\Omega} E y^m \, dA, \quad I_G^{(n)} := \int_{\Omega} G y^n \, dA, \tag{9}$$

with  $\Omega$  the two-dimensional domain modeling cross section. Terms in Eq. (9) are higher-order elastic stiffness coefficients (for  $m > 2, n > 0$ ), including bending stiffness  $I_E$  and shear stiffness  $A_G$  for  $m = 2$  and  $n = 0$ , respectively, i.e.,  $I_E^{(2)} := I_E$  and  $I_G^{(0)} := A_G$ . Hereinafter, the following notation will be adopted:

$$\begin{cases} \bar{I}_E := I_E - \alpha I_E^{(4)}, \\ \bar{I}_G^{(2)} := I_G^{(2)} - \beta I_G^{(4)}, \\ \bar{A}_G := A_G - \beta I_G^{(2)}, \\ \hat{A}_G := \bar{A}_G - \beta \bar{I}_G^{(2)}. \end{cases} \tag{10}$$

By reversing Eq. (8), we get the local elastic strains of the third-order beam model, that is:

$$\left\{ \begin{aligned} \bar{\varepsilon}^l(x) &= \frac{I_E^{(4)} P(x) - I_E^{(6)} M(x)}{(I_E^{(4)})^2 - I_E I_E^{(6)}}, \\ \bar{\bar{\varepsilon}}^l(x) &= \frac{I_E^{(4)} M(x) - I_E P(x)}{(I_E^{(4)})^2 - I_E I_E^{(6)}}, \\ \bar{\gamma}^l(x) &= \frac{I_G^{(2)} R(x) - I_G^{(4)} Q(x)}{(I_G^{(2)})^2 - A_G I_G^{(4)}}, \\ \bar{\bar{\gamma}}^l(x) &= \frac{I_G^{(2)} Q(x) - A_G R(x)}{(I_G^{(2)})^2 - A_G I_G^{(4)}}. \end{aligned} \right. \tag{11}$$

Then, manipulating system (11) we get

$$\left\{ \begin{aligned} P(x) &= \frac{I_E^{(4)}}{I_E} \left( M(x) - \alpha \frac{I_E^{(4)}}{\bar{A}_G} Q'(x) \right) + \alpha \frac{I_E^{(6)}}{\bar{A}_G} Q'(x), \\ R(x) &= \frac{\bar{I}_G^{(2)}}{\bar{A}_G} Q(x), \\ \bar{\varepsilon}^l(x) &= \frac{M(x)}{I_E} - \frac{\alpha I_E^{(4)} Q'(x)}{\bar{A}_G I_E}, \\ \bar{\gamma}^l(x) &= \frac{Q(x)}{\bar{A}_G}, \end{aligned} \right. \tag{12}$$

where all functional dependencies between strain fields in Eq. (4) have been taken into account. It is worth noting that equations (12)<sub>1,2</sub> provide elastic relations involving only stress fields while Eq. (12)<sub>3,4</sub> represent the effective constitutive relations.

Then, according to the stress-driven integral model [28], nonlocal elastic strains  $\{\bar{\varepsilon}, \bar{\gamma}\}$  are expressed as integral convolutions of the local elastic strains  $\{\bar{\varepsilon}^l, \bar{\gamma}^l\}$  and a proper averaging kernel  $\phi_{L_c}$  described by a characteristic length parameter  $L_c$ :

$$\left\{ \begin{aligned} \bar{\varepsilon}(x) &= (\phi_{L_c} * \bar{\varepsilon}^l)(x) := \int_0^L \phi_{L_c}(x - \xi) \left( \frac{M(\xi)}{I_E} - \frac{\alpha I_E^{(4)} Q'(\xi)}{\bar{A}_G I_E} \right) d\xi, \\ \bar{\gamma}(x) &= (\phi_{L_c} * \bar{\gamma}^l)(x) := \int_0^L \phi_{L_c}(x - \xi) \frac{Q(\xi)}{\bar{A}_G} d\xi. \end{aligned} \right. \tag{13}$$

Commonly adopted averaging kernels as originally proposed by Eringen in [6] are the error function

$$\phi_{L_c}^{err}(x) = \frac{1}{L_c \sqrt{\pi}} \exp\left(-\left(\frac{x}{L_c}\right)^2\right), \tag{14}$$

and the bi-exponential function (i.e., Helmholtz’s averaging kernel)

$$\phi_{L_c}^H(x) = \frac{1}{2 L_c} \exp\left(-\frac{|x|}{L_c}\right). \tag{15}$$

*Remark 1* The constitutive integral laws in Eq. (13) represent general expressions which lend themselves to any choice of the averaging kernel  $\phi_{L_c}$ . Adoption of different kernels in Eq. (13) leads to technically coincident structural responses as will be shown in Sect. 5. Thus, without loss of generality, choice of the bi-exponential kernel in Eq. (15) as done by Eringen in [6], is only more convenient for theoretical and computational purposes, by virtue of the peculiar properties it enjoys [18]. Indeed, if the Helmholtz’s kernel in Eq. (15) is adopted, the

integral equations (13) can be expressed in an equivalent differential formulation [28] so that nonlocal elastic strains  $\{\bar{\varepsilon}, \bar{\gamma}\}$  can be obtained as the unique solution of the following second-order differential equations

$$\begin{cases} \bar{\varepsilon}(x) - L_c^2 \bar{\varepsilon}''(x) = \frac{M(x)}{I_E} - \frac{\alpha I_E^{(4)} Q'(x)}{\bar{A}_G I_E}, \\ \bar{\gamma}(x) - L_c^2 \bar{\gamma}''(x) = \frac{Q(x)}{\bar{A}_G}, \end{cases} \tag{16}$$

equipped with the constitutive boundary conditions

$$\begin{cases} \bar{\varepsilon}'(0) = \frac{\bar{\varepsilon}(0)}{L_c}, \quad \bar{\varepsilon}'(L) = -\frac{\bar{\varepsilon}(L)}{L_c}, \\ \bar{\gamma}'(0) = \frac{\bar{\gamma}(0)}{L_c}, \quad \bar{\gamma}'(L) = -\frac{\bar{\gamma}(L)}{L_c}. \end{cases} \tag{17}$$

*Remark 2* Let us rearrange Eq. (12) as follows:

$$\begin{cases} \bar{\varepsilon}^l(x) = \frac{M(x)}{I_E} - \frac{\alpha I_E^{(4)} Q'(x)}{\bar{A}_G I_E} = \frac{P(x)}{I_E^{(4)}} - \alpha \frac{I_E^{(6)}}{\bar{A}_G I_E^{(4)}} Q'(x), \\ \bar{\gamma}^l(x) = \frac{Q(x)}{\bar{A}_G} = \frac{R(x)}{\bar{I}_G^{(2)}}. \end{cases} \tag{18}$$

Then, the nonlocal elastic strain fields  $\{\bar{\varepsilon}, \bar{\gamma}\}$  are obtained by the stress-driven integral convolutions in Eq. (13), that is

$$\begin{cases} \bar{\varepsilon} = \phi_{L_c} * \left( \frac{M}{I_E} - \frac{\alpha I_E^{(4)} Q'}{\bar{A}_G I_E} \right) = \phi_{L_c} * \left( \frac{P}{I_E^{(4)}} - \alpha \frac{I_E^{(6)}}{\bar{A}_G I_E^{(4)}} Q' \right), \\ \bar{\gamma} = \phi_{L_c} * \frac{Q}{\bar{A}_G} = \phi_{L_c} * \frac{R}{\bar{I}_G^{(2)}}. \end{cases} \tag{19}$$

By linearity of the operator  $\phi_{L_c} *$ , from Eq. (19) we get

$$\begin{cases} \phi_{L_c} * \left( \frac{M}{I_E} - \frac{\alpha I_E^{(4)} Q'}{\bar{A}_G I_E} - \frac{P}{I_E^{(4)}} + \alpha \frac{I_E^{(6)}}{\bar{A}_G I_E^{(4)}} Q'(x) \right) = 0, \\ \phi_{L_c} * \left( \frac{Q}{\bar{A}_G} - \frac{R}{\bar{I}_G^{(2)}} \right) = 0. \end{cases} \tag{20}$$

Equation (20) implies that source fields are zero functions. Thus, Eq. (12)<sub>1,2</sub> still hold and therefore can be adopted to formulate the nonlocal elastic equilibrium problem of third-order beams, as shown in the following.

#### 4 Nonlocal elastic equilibrium of third-order beams

The stress-driven nonlocal elastostatic problem of third-order beams is formulated below along with the adopted analytical solution procedure which is illustrated in detail.

Let us rewrite the differential equilibrium conditions in Eq. (6) as follows:

$$\begin{cases} M''(x) = q(x), \\ M'(x) - \alpha P'(x) = \beta R(x) - Q(x). \end{cases} \tag{21}$$

Then, substituting  $P$  (Eq. (12)<sub>1</sub>) and  $R$  (Eq. (12)<sub>2</sub>) in the equilibrium equation (21)<sub>2</sub>, we get the second-order differential equation in the unknown field  $Q$

$$\alpha^2 \left( \frac{(I_E^{(4)})^2}{I_E \bar{A}_G} - \frac{I_E^{(6)}}{\bar{A}_G} \right) Q''(x) + \frac{\hat{A}_G}{\bar{A}_G} Q(x) + \frac{\bar{I}_E}{I_E} M'(x) = 0 \tag{22}$$

where  $M'(x) = \int_0^x q(\xi) d\xi + C$  from Eq. (21)<sub>1</sub>, with  $C$  the integration constant. The differential equilibrium equations (21)<sub>1</sub>–(22) have to be solved with prescription of proper static boundary conditions.

Then, nonlocal elastic strain fields are provided by the constitutive integral laws in Eq. (13):

$$\begin{cases} \bar{\varepsilon}(x) = \int_0^L \phi_{L_c}(x - \xi) \left( \frac{M(\xi)}{I_E} - \frac{\alpha I_E^{(4)} Q'(\xi)}{\bar{A}_G I_E} \right) d\xi, \\ \bar{\gamma}(x) = \int_0^L \phi_{L_c}(x - \xi) \frac{Q(\xi)}{\bar{A}_G} d\xi. \end{cases} \tag{23}$$

Finally, shape-functions  $w$  and  $\varphi$  are obtained by prescribing differential kinematic compatibility equations

$$\begin{cases} \bar{\varepsilon}(x) = \varphi'(x), \\ \bar{\gamma}(x) = w'(x) - \varphi(x) \end{cases} \tag{24}$$

equipped with kinematic boundary conditions.

The case studies illustrated in the next section involve prescription of the following boundary conditions

$$\begin{cases} \text{Free :} & M' = 0, \quad P = 0, \quad M = 0; \\ \text{Hinge :} & w = 0, \quad P = 0, \quad M = 0; \\ \text{Clamp :} & w = 0, \quad w' = 0, \quad \varphi = 0; \end{cases} \tag{25}$$

that can be directly deduced from Eq. (7). It is worth noting that, from Eq. (12)<sub>1</sub>, the conditions  $P = M = 0$  also imply  $Q' = 0$ .

As shown in Sects. 3 and 4, the relevant nonlocal elastic equilibrium problem of third-order beams based on the stress-driven model is well-posed. The conclusion amends recent claims in [34] concerning ill-posedness of the elastostatic problem of stress-driven nonlocal third-order beams.

### 5 Case studies

Analytical solutions obtained by applying the procedure illustrated in Sect. 4 are here presented for exemplar structural schemes of technological interest.

For this purpose, let us consider a third-order beam of length  $L$  having a rectangular cross section with height  $h = 0.2L$  and base  $b = 0.5h$ . The beam is assumed to be made of silicon carbide, with Euler–Young modulus  $E = 380$  [GPa] and Poisson’s ratio  $\nu = 0.3$  [11]. Parametric solutions are obtained for increasing nonlocal parameter  $\lambda = L_c/L$ . For  $\lambda \rightarrow 0^+$  solutions of local elastic equilibrium problems of third-order beams are recovered. In the following, the beam length is assumed to be  $L = 50$  [nm].

#### 5.1 Cantilever (CF) beam under uniformly distributed transverse loading

A uniformly distributed transverse loading  $q = 10^{-2}$  [nN/nm] is applied. Clamped end at  $x = 0$  requires essential boundary conditions (BCs)  $w = \varphi = w' = 0$ .

Free end at  $x = L$  prescribes  $M' = M = P = 0$  where the last two BCs provide  $Q' = 0$ . Solution of equilibrium equation  $M'' = q$  with natural boundary conditions  $M(L) = M'(L) = 0$  yields  $M(x) = q(L - x)^2/2$ . Then, the second-order differential equation (22) equipped with natural boundary condition  $Q'(L) = 0$  is solved to get the unknown field  $Q$  as function of the integration constant  $c_Q$ . The nonlocal strain fields  $\bar{\varepsilon}$  and  $\bar{\gamma}$  are obtained by the integral convolutions in Eq. (23) where the Helmholtz’s averaging kernel Eq. (15) is adopted. Finally, differential kinematic compatibility system of Eq. (24) is solved by prescribing

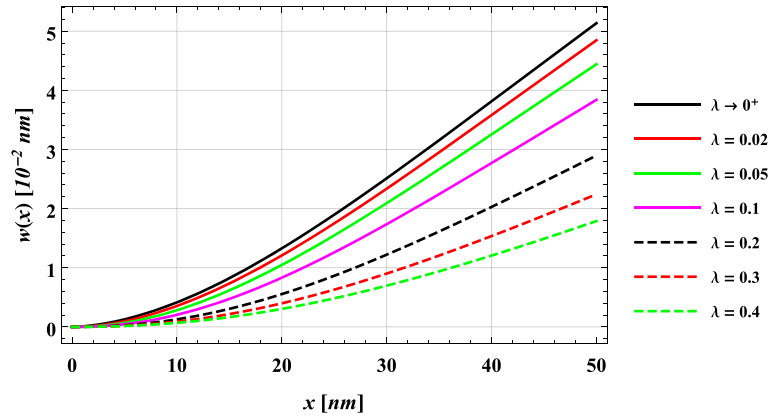


**Fig. 1** Cantilever beam under uniformly distributed transverse loading: shape-function  $w(x)$  [ $10^{-2}$  nm] versus  $x$  [nm] for  $\lambda = \{0^+, 0.02, 0.05, 0.1, 0.2, 0.3, 0.4\}$

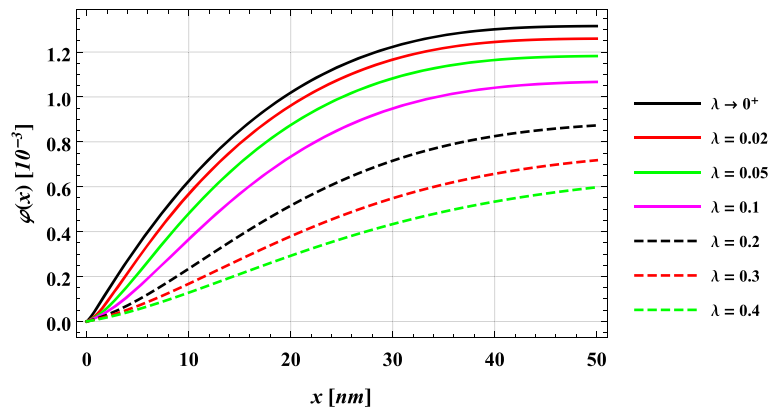


**Fig. 2** Cantilever beam under uniformly distributed transverse loading: shape-function  $\varphi(x)$  [ $10^{-3}$ ] versus  $x$  [nm] for  $\lambda = \{0^+, 0.02, 0.05, 0.1, 0.2, 0.3, 0.4\}$

kinematic boundary conditions  $\varphi(0) = w(0) = 0$ , while kinematic boundary condition  $w'(0) = 0$  is prescribed to get the unknown integration constant  $c_Q$ .

Plots of the solution fields are depicted in Figs. 1 and 2. The parametric analysis shows a stiffening behavior of structural responses for increasing nonlocal parameter  $\lambda$ . The shear stress fields on the cross section at  $x = L/2$  are parametrically represented in Fig. 3 for increasing  $\lambda$ .

### 5.2 Simply supported (SS) beam under uniformly distributed transverse loading

A uniformly distributed transverse loading  $q = 10^{-1}$  [nN/nm] is applied. Pinned ends require  $w(x_i) = P(x_i) = M(x_i) = 0$  for  $i = \{1, 2\}$ . The last two boundary conditions also imply  $Q'(x_i) = 0$ . Then, equilibrium differential equation  $M'' = q$  with natural boundary conditions  $M(0) = M(L) = 0$  yields  $M(x) = q(x - L)x/2$ . Solution of the second-order differential equation (22) equipped with boundary conditions  $Q'(0) = Q'(L) = 0$  provides the unknown field  $Q$ . Nonlocal strain fields  $\bar{\epsilon}$  and  $\bar{\gamma}$  are obtained by the integral convolutions in Eq. (23) where the Helmholtz's averaging kernel Eq. (15) is adopted. Finally, differential kinematic compatibility system (24) is solved by prescribing kinematic boundary conditions  $w(0) = w(L) = 0$ .

Parametric plots of solution fields are shown in Figs. 4 and 5, showing stiffening responses for increasing nonlocal parameter  $\lambda$ . Shear stress fields on cross section at  $x = L$  are parametrically represented in Fig. 6 for increasing nonlocal parameter  $\lambda$ .

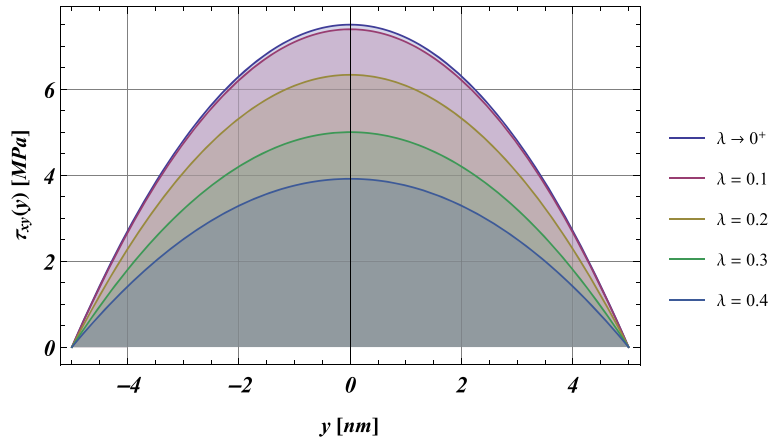


**Fig. 3** Cantilever beam under uniformly distributed transverse loading: shear stress field  $\tau_{xy}(y)$  [MPa] versus  $y$  [nm] at mid-span for  $\lambda = \{0^+, 0.1, 0.2, 0.3, 0.4\}$

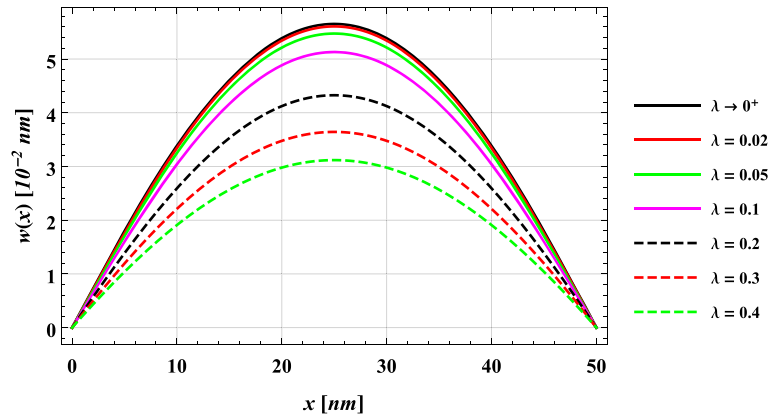


**Fig. 4** Simply supported beam under uniformly distributed transverse loading: shape-function  $w(x)$  [ $10^{-2}$  nm] versus  $x$  [nm] for  $\lambda = \{0^+, 0.02, 0.05, 0.1, 0.2, 0.3, 0.4\}$

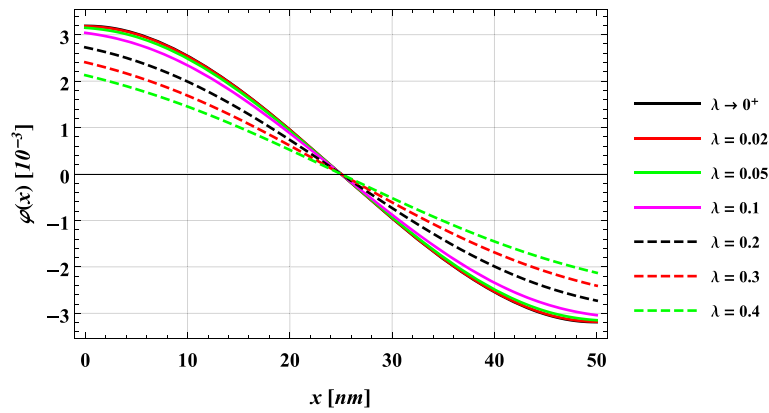


**Fig. 5** Simply supported beam under uniformly distributed transverse loading: shape-function  $\varphi(x)$  [ $10^{-3}$ ] versus  $x$  [nm] for  $\lambda = \{0^+, 0.02, 0.05, 0.1, 0.2, 0.3, 0.4\}$



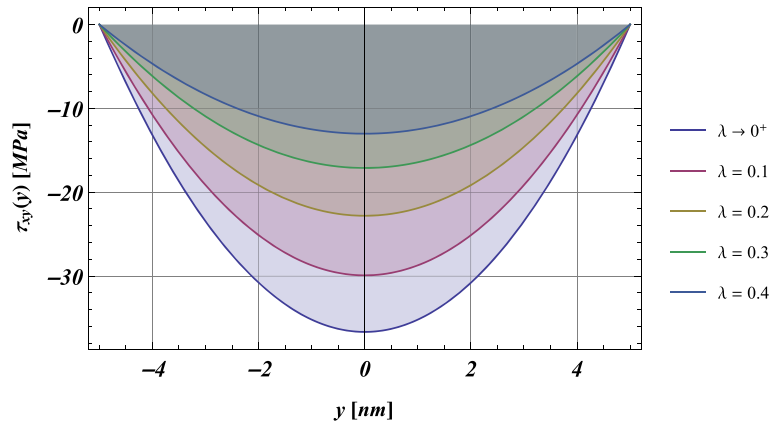


**Fig. 6** Simply supported beam under uniformly distributed transverse loading: shear stress field  $\tau_{xy}(y)$  [MPa] versus  $y$  [nm] at free end for  $\lambda = \{0^+, 0.1, 0.2, 0.3, 0.4\}$

**Table 1** Cantilever beam: nonlocal responses for the error kernel  $\phi_\lambda^{err}$  and the Helmholtz kernel  $\phi_\lambda^H$

$\lambda$	$w(L)$ [ $10^{-2}$ nm]		$\varphi(L)$ [ $10^{-3}$ ]	
	$\phi_\lambda = \phi_\lambda^{err}$	$\phi_\lambda = \phi_\lambda^H$	$\phi_\lambda = \phi_\lambda^{err}$	$\phi_\lambda = \phi_\lambda^H$
0.05	4.6901	4.4407	1.2292	1.1820
0.10	4.2517	3.8392	1.1442	1.0669
0.20	4.1925	2.8966	1.1398	0.8731
0.30	3.7417	2.2423	1.0674	0.7180
0.40	3.3402	1.7887	0.9966	0.5974

**Table 2** Simply supported beam: nonlocal responses for the error kernel  $\phi_\lambda^{err}$  and the Helmholtz kernel  $\phi_\lambda^H$

$\lambda$	$w(L/2)$ [ $10^{-2}$ nm]		$\varphi(0)$ [ $10^{-3}$ ]	
	$\phi_\lambda = \phi_\lambda^{err}$	$\phi_\lambda = \phi_\lambda^H$	$\phi_\lambda = \phi_\lambda^{err}$	$\phi_\lambda = \phi_\lambda^H$
0.05	5.5857	5.4739	3.1793	3.1489
0.10	5.4620	5.1298	3.1483	3.0405
0.20	5.0788	4.3259	3.0319	2.7273
0.30	4.5832	3.6432	2.8615	2.4058
0.40	4.0670	3.1182	2.6592	2.1274

### 5.3 Averaging kernel: bi-exponential versus error function

The elastic equilibrium problem illustrated in Sect. 4 is formulated exploiting the nonlocal integral laws in Eq. (13), equipped with any averaging kernel fulfilling symmetry, positivity and limit impulsivity [6].

For comparison sake, results obtained in Sect. 5 by adopting as averaging kernel the bi-exponential (Helmholtz's) function  $\phi_\lambda^H$  in Eq. (15), are here analyzed with respect to those obtained by exploiting the error function  $\phi_\lambda^{err}$  in Eq. (14). Structural responses for increasing nonlocal parameter  $\lambda$  are shown in Tables 1 and 2 for cantilever and simply supported beams analyzed in Sect. 5. Notably, Tables 1 and 2 show that for  $\lambda < 0.2$ , results got by exploiting different kernels are technically coincident.

### 5.4 Validation of results

Solutions of the local elastic equilibrium problem can be recovered as limiting cases of the nonlocal elastostatic problem formulated in Sect. 4. Indeed, nonlocal shape-functions  $w, \varphi$  of the examined case studies for  $\lambda \rightarrow 0^+$  (see Table 3) perfectly match the local elastic results provided in [24].

**Table 3** Limiting solutions of nonlocal elastic equilibrium problems for  $\lambda \rightarrow 0$ 

x [nm]	CF		SS	
	w(x) [10 <sup>-2</sup> nm]	$\varphi(x)$ [10 <sup>-3</sup> ]	w(x) [10 <sup>-2</sup> nm]	$\varphi(x)$ [10 <sup>-3</sup> ]
0	0.000	0.000	0.000	3.189
5	0.127	0.338	1.798	3.023
10	0.414	0.626	3.381	2.544
15	0.824	0.850	4.610	1.827
20	1.327	1.019	5.387	0.953
25	1.897	1.141	5.652	0.000
30	2.513	1.223	5.387	- 0.953
35	3.156	1.274	4.610	- 1.827
40	3.814	1.301	3.381	- 2.544
45	4.475	1.312	1.798	- 3.023
50	5.135	1.316	0.000	- 3.189

## 6 Closing remarks

Stress-driven theory of nonlocal elasticity has been adopted to model size effects in third-order shear deformable beams. Kinematics and equilibrium of the third-order model have been illustrated; then, the stress-driven integral model has been extended to third-order elastic beams and an equivalent differential formulation with nonclassical boundary conditions has been derived. The corresponding nonlocal elastic equilibrium problem of third-order small-scale beams has been formulated and addressed by an effective analytical methodology. Parametric closed-form nonlocal structural solutions of exemplar case-problems of applied interest have been established, examined and validated. According to the proposed beam model, there is no need to evaluate shear correction factors, which is a crucial point in the framework of nonlocal elasticity. Thus, by combining the stress-driven elasticity with the third-order beam theory, the presented methodology provides an effective approach to capture the size-dependent behavior of small-scale beams.

As emerged from the parametric studies, a stiffening mechanical behavior has been predicted by the presented approach in agreement with experimental outcomes in [1,9], thus confirming the peculiar mechanical phenomenon of *smaller-is-stiffer*.

**Acknowledgements** Financial supports from MIUR in the framework of the Project PRIN 2017—code 2017J4EAYB Multiscale Innovative Materials and Structures (MIMS)—University of Naples Federico II Research Unit and from the research program ReLUIS 2021 are gratefully acknowledged.

**Funding** Open access funding provided by Università degli Studi di Napoli Federico II within the CRUI-CARE Agreement.

**Open Access** This article is licensed under a Creative Commons Attribution 4.0 International License, which permits use, sharing, adaptation, distribution and reproduction in any medium or format, as long as you give appropriate credit to the original author(s) and the source, provide a link to the Creative Commons licence, and indicate if changes were made. The images or other third party material in this article are included in the article's Creative Commons licence, unless indicated otherwise in a credit line to the material. If material is not included in the article's Creative Commons licence and your intended use is not permitted by statutory regulation or exceeds the permitted use, you will need to obtain permission directly from the copyright holder. To view a copy of this licence, visit <http://creativecommons.org/licenses/by/4.0/>.

## References

1. Abazari, A.M., Safavi, S.M., Rezazadeh, G., Villanueva, L.G.: Modelling the size effects on the mechanical properties of micro/nano structures. *Sensors* **15**(11), 28543–28562 (2015)
2. Acierno, S., Barretta, R., Luciano, R., Marotti de Sciarra, F., Russo, P.: Experimental evaluations and modeling of the tensile behavior of polypropylene/single-walled carbon nanotubes fibers. *Compos. Struct.* **174**, 12–18 (2017)
3. Bickford, W.B.: A consistent higher order beam theory. *Dev. Theor. Appl. Mech.* **11**, 137–150 (1982)
4. Darban, H., Caporale, A., Luciano, R.: Nonlocal layerwise formulation for bending of multilayered/functionally graded nanobeams featuring weak bonding. *Eur. J. Mech. A/Solids* **86**, 104193 (2021)
5. Eringen, A.C.: Linear theory of nonlocal elasticity and dispersion of plane waves. *Int. J. Eng. Sci.* **10**, 425–435 (1972)
6. Eringen, A.C.: On differential equations of nonlocal elasticity and solutions of screw dislocation and surface waves. *J. Appl. Phys.* **54**(9), 4703–4710 (1983)
7. Eringen, A.C.: Theory of nonlocal elasticity and some applications. *Res. Mech.* **21**, 313–342 (1987)

8. Farajpour, A., Howard, C.Q., Robertson, W.S.P.: On size-dependent mechanics of nanoplates. *Int. J. Eng. Sci.* **156**, 103368 (2020)
9. Fuschi, P., Pisano, A., Polizzotto, C.: Size effects of small-scale beams in bending addressed with a strain-difference based nonlocal elasticity theory. *Int. J. Mech. Sci.* **151**, 661–671 (2019)
10. Heyliger, P.R., Reddy, J.N.: A higher-order beam finite element for bending and vibration problems. *J. Sound Vib.* **126**, 309–326 (1988)
11. Jankowski, P., Żur, K.K., Kim, J., Reddy, J.: On the bifurcation buckling and vibration of porous nanobeams. *Compos. Struct.* **250**, 112632 (2020)
12. Kröner, E.: Elasticity theory of materials with long range cohesive forces. *Int. J. Solids Struct.* **3**(5), 731–742 (1967)
13. Levinson, M.: A new rectangular beam theory. *J. Sound Vib.* **74**(1), 81–87 (1981)
14. Luciano, R., Willis, J.: Non-local constitutive response of a random laminate subjected to configuration-dependent body force. *J. Mech. Phys. Solids* **49**(2), 431–444 (2001)
15. Luciano, R., Willis, J.: FE analysis of stress and strain fields in finite random composite bodies: application to crack tip field. In: 11th International Conference on Fracture 2005, ICF11, vol. 1 (2005)
16. Malikan, M., Eremeyev, V.A., Żur, K.K.: Effect of axial porosities on flexomagnetic response of in-plane compressed piezomagnetic nanobeams. *Symmetry* **12**(12), 255 (2020)
17. Penna, R., Feo, L., Fortunato, A., Luciano, R.: Nonlinear free vibrations analysis of geometrically imperfect FG nano-beams based on stress-driven nonlocal elasticity with initial pretension force. *Compos. Struct.* **255**, 112856 (2021)
18. Pisano, A., Fuschi, P., Polizzotto, C.: Integral and differential approaches to Eringen's nonlocal elasticity models accounting for boundary effects with applications to beams in bending. *ZAMM J. Appl. Math. Mech.* (2021). <https://doi.org/10.1002/zamm.202000152>
19. Pourasghar, A., Chen, Z.: Effect of hyperbolic heat conduction on the linear and nonlinear vibration of CNT reinforced size-dependent functionally graded microbeams. *Int. J. Eng. Sci.* **137**, 57–72 (2019)
20. Reddy, J.N.: A simple higher-order theory for laminated composite plates. *J. Appl. Mech.* **51**(4), 745–752 (1984)
21. Reddy, J.N.: A review of the literature on finite-element modeling of laminated composite plates. *Shock Vib. Dig.* **17**(4), 3–8 (1985)
22. Reddy, J.N.: *Energy Principles and Variational Methods in Applied Mechanics*, 2nd edn. Wiley, New York (2002)
23. Reddy, J.N.: *Theories and Analyses of Beams and Axisymmetric Circular Plates*. Taylor & Francis, CRC Press, Philadelphia (2022) (to appear)
24. Reddy, J.N., Wang, C.M., Lee, K.H.: Relationships between bending solutions of classical and shear deformation beam theories. *Int. J. Solids Struct.* **34**(26), 3373–3384 (1997)
25. Roghani, M., Rouhi, H.: Nonlinear stress-driven nonlocal formulation of Timoshenko beams made of FGMs. *Contin. Mech. Thermodyn.* **33**, 343–355 (2021)
26. Rogula, D.: Influence of spatial acoustic dispersion on dynamical properties of dislocations. *Bull. Pol. Acad. Sci. Tech. Sci.* **13**, 337–385 (1965)
27. Rogula, D.: *Introduction to Nonlocal Theory of Material Media*, pp. 123–222. Springer, Vienna (1982)
28. Romano, G., Barretta, R.: Nonlocal elasticity in nanobeams: the stress-driven integral model. *Int. J. Eng. Sci.* **115**, 14–27 (2017)
29. Romano, G., Barretta, R., Diaco, M., Marotti de Sciarra, F.: Constitutive boundary conditions and paradoxes in nonlocal elastic nanobeams. *Int. J. Mech. Sci.* **121**, 151–156 (2017)
30. Romano, G., Diaco, M.: On formulation of nonlocal elasticity problems. *Meccanica* **56**, 1303–1328 (2020)
31. Sedighi, H.M., Malikan, M.: Stress-driven nonlocal elasticity for nonlinear vibration characteristics of carbon/boron-nitride hetero-nanotube subject to magneto-thermal environment. *Phys. Scr.* **95**(5), 055218 (2020)
32. Soukari, D., Ecochard, V., Salom, L.: DNA-based nanobiosensors for monitoring of water quality. *Int. J. Hyg. Environ. Health* **226**, 113485 (2020)
33. Udara, S., Krishnamurthy Revankar, P.: Sensitivity and selectivity enhancement of MEMS/NEMS cantilever by coating of Polyvinylpyrrolidone. *Mater. Today Proc.* **18**, 1610–1619 (2019)
34. Zhang, P., Qing, H.: On well-posedness of two-phase nonlocal integral models for higher-order refined shear deformation beams. *Appl. Math. Mech.* **42**, 931–950 (2021)
35. Zhang, P., Qing, H., Gao, C.F.: Exact solutions for bending of Timoshenko curved nanobeams made of functionally graded materials based on stress-driven nonlocal integral model. *Compos. Struct.* **245**, 112362 (2020)